

## Pressure dependence of photoluminescence in $\text{In}_x\text{Ga}_{1-x}\text{As}/\text{GaAs}$ strained quantum wells

H. Q. Hou,\* L. J. Wang, R. M. Tang, and J. M. Zhou

*Institute of Physics, Chinese Academy of Sciences, Beijing 100 080, People's Republic of China*

(Received 20 February 1990; revised manuscript received 23 April 1990)

Photoluminescence properties of  $\text{In}_x\text{Ga}_{1-x}\text{As}/\text{GaAs}$  strained quantum wells with well widths from 13 to 120 Å are investigated as a function of hydrostatic pressure (0–45 kbar) at liquid-nitrogen temperature. Pressure coefficients of the  $E_{\Gamma_h}^{\uparrow}$  transitions between the quantized ground levels of the  $\Gamma$  conduction band and the heavy-hole valence band are presented. A weak recombination with a pressure coefficient of  $-2.6$  meV/kbar is identified, which is attributable to the transition related to the crossover of the  $\Gamma$  band in the well layer and the  $X$  band in the barrier layer. Correlating this transition to barrier-to-well indirect recombination, the valence-band-offset fraction is given as  $Q_v = \Delta E_v / (\Delta E_v + \Delta E_c) = 0.32$  for a sample with indium fraction of  $x = 0.25$ . The light-hole band is, therefore, inferred to be type II. Furthermore, the pressure coefficient is found to increase with decreasing well widths, which is opposite to that observed in the  $\text{GaAs}/(\text{Al,Ga})\text{As}$  quantum-well system. A calculation based on the envelope-function model is made to interpret this dependence.

### I. INTRODUCTION

There is growing interest in strained-layer semiconductor heterostructures, in which the lattice mismatch between layers can be accommodated by coherent elastic strain,<sup>1</sup> provided that the layer thicknesses are within the critical layer thickness.<sup>2</sup> The electronic states in these types of heterostructures are modulated both by the strain and by the periodic potential along the growth direction ( $z$  axis). The possibility of getting high-quality samples with large lattice mismatches has provided new prospects for modern materials science. As a result, the electronic structure of strained quantum wells (SQW's), such as  $\text{In}_x\text{Ga}_{1-x}\text{As}/\text{GaAs}$  quantum wells, has been frequently studied.<sup>3–11</sup>

Hydrostatic pressure has been shown to be a valuable perturbation technique for studying the electronic properties of two-dimensional semiconductor materials.<sup>10–16</sup> However, work to date has concentrated on the  $\text{GaAs}/\text{Al}_x\text{Ga}_{1-x}\text{As}$  system,<sup>12–15,17–21</sup> with relatively little work on SQW structures.<sup>10,11,16</sup> A pressure, especially a uniaxial pressure applied along the  $z$  direction, can be used efficiently to probe the strain-induced band structure.<sup>17,18</sup> Photoluminescence (PL) measurements were made at a temperature of 77 K for various  $\text{In}_x\text{Ga}_{1-x}\text{As}/\text{GaAs}$  SQW's under hydrostatic pressure. The energy of excitonic transitions were found to be strongly dependent on the pressure; a weak recombination was observed, attributable to a pressure-induced crossover of the  $\Gamma$  band in the well layer and the  $X$  conduction band in the barrier layer. The valence-band offset is deduced and the pressure coefficients and their dependence on the well width were determined. A theoretical calculation based on the envelope-function model is used to interpret the pressure-coefficient dependence on the well width.

### II. EXPERIMENTAL DETAILS

The samples used in this study were prepared by a computer-controlled molecular-beam-epitaxy machine made in China. The indium composition and layer thickness were deduced from reflection high-energy electron diffraction (RHEED) intensity oscillations, and are in good agreement with double crystal x-ray diffraction measurements<sup>22</sup> on multiple-quantum-well samples grown under identical conditions. The uncertainties for the fractional alloy composition and layer thickness are  $\pm 0.005$  and  $\pm 5$  Å, respectively. Sample 1 is composed of two  $\text{In}_{0.25}\text{Ga}_{0.75}\text{As}/\text{GaAs}$  SQW's with well widths of 13 and 22 Å and two  $\text{GaAs}/\text{Al}_{0.3}\text{Ga}_{0.7}\text{As}$  quantum wells (QW's) with well widths of 23 and 45 Å. The  $\text{In}_x\text{Ga}_{1-x}\text{As}$  SQW's were grown adjacent to the sample surface, while the two  $\text{GaAs}/\text{Al}_x\text{Ga}_{1-x}\text{As}$  QW's lie deeper within the structure. Sample 2 consists of five  $\text{In}_{0.16}\text{Ga}_{0.84}\text{As}$  wells with a well-width sequence of 120, 90, 65, 40, and 20 Å along the growth direction. All the QW's were separated by 150-Å barrier layers to prevent coupling between wells. Transmission-electron-microscopy (TEM) measurements show the samples to be free of dislocations at the interfaces.<sup>22</sup>

For pressure application, the samples were thinned to about 60  $\mu\text{m}$  from the backside, and cleaved into squares with sides of less than 0.2 mm. A single sample and a fine ruby particle were placed in a gasketed diamond-anvil cell (DAC). A 4:1 mixture of methanol and ethanol was used as the pressure-transmitting fluid. The pressure was determined by monitoring the shift in the  $R(1)$  emission from the ruby particle. The transmitting mixture was observed to be in a glasslike state at 77 K, and the hydrostatic character was inferred to be better than  $\pm 0.2$  kbar, measured from several ruby chips placed at various positions in the pressure cell.<sup>11</sup> The DAC was immersed into

liquid nitrogen, but the changes in pressure were only made at room temperature to ensure hydrostatic conditions. The temperature and pressure were observed to be stable throughout the entire experiment. PL measurements were performed using the 5145-Å radiation line from an argon-ion laser, and dispersed by a double-grating spectrometer with a microfocusing device. The signal was acquired by a photon-counting system and processed by a computer. A GaAs cathode photomultiplier tube was used as the detector. The spectral resolution was 3 Å.

### III. RESULTS AND DISCUSSIONS

#### A. Pressure coefficients

The inset of Fig. 1 is a schematic diagram of the conduction band in the quantum structure of sample 1. The PL spectra at 77 K and normal pressure are presented in Fig. 1(a). Transitions ( $E_{lh}^{\Gamma}$ ) between the  $n=1$  electron level in the conduction band (CB) and the  $n=1$  heavy-hole (HH) subband in the valence band (VB) were observed for each QW. Transitions corresponding to various wells are labeled with the same letters. Peak *E* corresponds to the exciton transition from the GaAs buffer layer. The GaAs/ $\text{Al}_x\text{Ga}_{1-x}\text{As}$  QW's in sample 1 were grown to aid the determination of the GaAs growth rate. Since the optical and pressure behaviors of GaAs/ $\text{Al}_x\text{Ga}_{1-x}\text{As}$  QW's are already well known,<sup>12-15</sup> these QW's will help confirm the pressure as calibrated

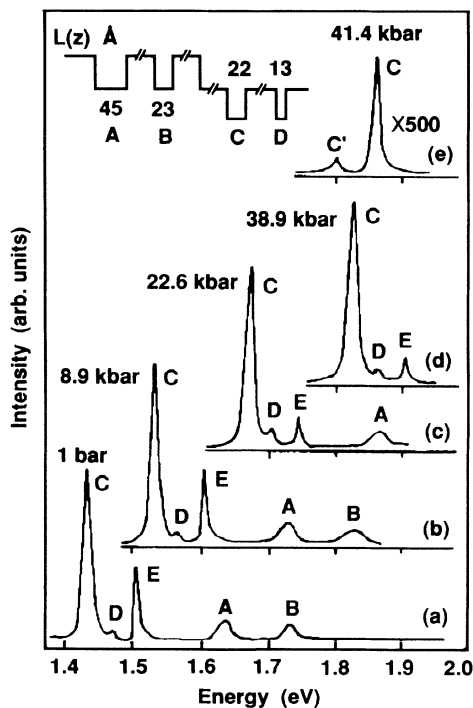


FIG. 1. PL spectra of sample 1 at 77 K and several values of pressure. The conduction band of the sample structure is schematically shown in the inset. PL peaks are indicated with the same letters as the corresponding quantum wells. Peak *E* is the exciton transition from the GaAs buffer layer.

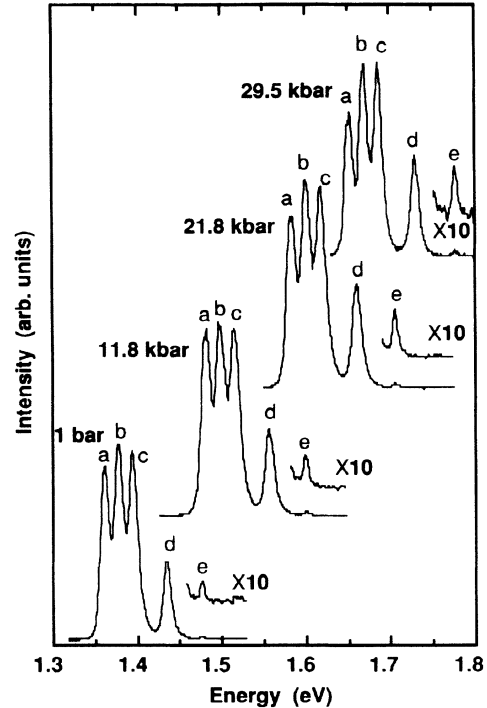


FIG. 2. PL spectra of sample 2 at 77 K and several values of pressure.

by the ruby chip. PL emissions from these two QW's were partially absorbed by the SQW's, which are situated nearer to the surface. The weak PL intensity resulting from QW *D* is attributed to its narrow well width (13 Å); the excitons inside it are strongly scattered by defects at the  $\text{In}_x\text{Ga}_{1-x}\text{As}/\text{GaAs}$  interfaces. The electron-to-light-hole transition cannot be observed in these two samples because the splitting generated by the

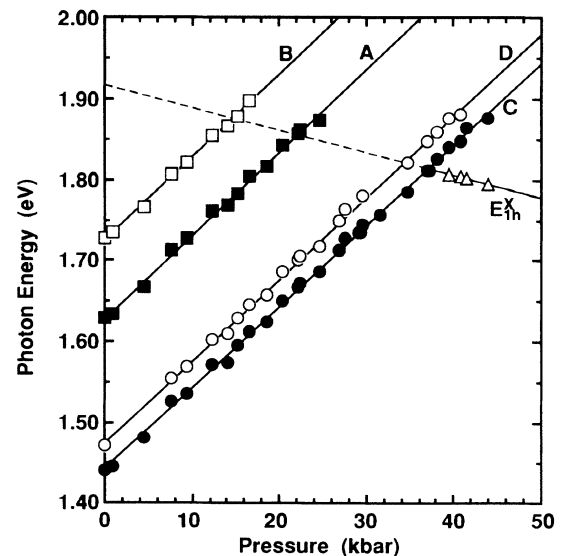


FIG. 3. Photon energy of  $E_{lh}^{\Gamma}$  emissions as a function of the pressure for quantum wells *A*–*D* in sample 1 at 77 K. The solid lines are linear least-squares fits to the data.

TABLE I. Pressure coefficients for samples 1 and 2 as determined experimentally.

	Sample No.									
	1					2				
Well material	In <sub>0.25</sub> Ga <sub>0.75</sub> As					GaAs				
Well widths (Å)	13	22	23	45	bulk	20	40	65	90	120
$\alpha$ (meV/kbar)	10.1	10.0	10.2	10.3	10.6	10.51	10.25	10.03	9.98	9.94

built-in biaxial strains causes the light-hole band to be far away from the heavy-hole band.<sup>3-8</sup> Figures 1(b)–1(e) show the PL spectra under various hydrostatic-pressure values at 77 K. With increasing pressure, all the PL peaks shift up in energy due to the pressure-induced gap shift of the bulk GaAs. The emission intensity decreases drastically for the narrow well at high pressure due to the CB crossover, which will be described in detail later.

Figure 2 shows corresponding PL results at different pressures for sample 2. The peaks are related to the HH exciton emissions from the five quantum wells, all of different well width. PL intensities in the spectra were corrected by the response efficiency of the detection system, since the quantum efficiency of the photomultiplier decreases in the long-wavelength region.

The dependence of the transition energy on pressure for each QW is plotted in Figs. 3 and 4 for samples 1 and 2, respectively. Since the band gaps of GaAs and InAs are proportionally dependent on the pressure,<sup>23</sup> a least-squares fit was employed for each set of data using the linear function:

$$E_{1h}^{\Gamma}(P) = E_{1h}^{\Gamma}(0) + \alpha P, \quad (1)$$

where energy  $E$  is in eV and pressure  $P$  is in kbar. The pressure coefficients obtained from the line slopes are listed in Table I.

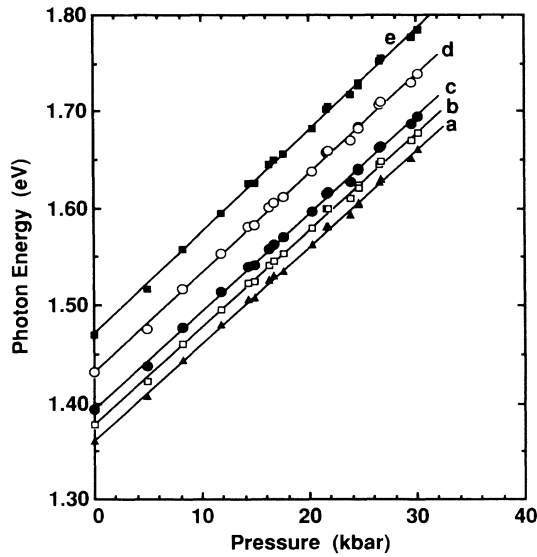


FIG. 4. Photon energy of  $E_{1h}^{\Gamma}$  emissions as a function of the pressure for wells a–e having widths  $a=120$  Å,  $b=90$  Å,  $c=65$  Å,  $d=40$  Å, and  $e=20$  Å in sample 2 at 77 K. The solid lines are linear least-squares fits to the data.

To ensure the accuracy of the determination of pressure and photon energy, the experiment was performed from 1 bar to 40 kbar with two runs. The uncertainties in pressure and emission energy were determined to be  $\pm 0.2$  kbar and  $\pm 1$  meV, respectively, which results in an experimental uncertainty in the pressure coefficient of  $\pm 1\%$ . Assuming that the pressure coefficient of the In<sub>x</sub>Ga<sub>1-x</sub>As SQW results mainly from the pressure-induced enlargement of the In<sub>x</sub>Ga<sub>1-x</sub>As band gap, and that this value can be linearly interpolated from those of GaAs and InAs, it may be concluded that the pressure coefficient of InAs is smaller than that of GaAs. This result is consistent with the original ones obtained for bulk materials.<sup>23</sup>

#### B. Energy-level crossover and valence-band offset

It can be seen from Fig. 1 that the PL intensity from all the QW's decreases drastically with increasing pressure. For sample 1 this occurs first for the narrowest well (located at higher energy), and is followed in succession by the larger well widths, which eventually vanish one after another as the pressure is increased. PL emissions from GaAs/Al<sub>x</sub>Ga<sub>1-x</sub>As QW's are the first to disappear since the initial emission intensities are very low. The spectrum for sample 1 at 41.4 kbar is illustrated in Fig. 1(e). A new peak of weaker intensity at a lower energy than the transition  $E_{1h}^{\Gamma}$  from quantum well C is observable when the pressure is increased to a value greater than a critical value  $P_c$ . This new peak is labeled C' in Fig. 1(e) and is related to the transition  $E_{1h}^X$ . The photon energies of the  $E_{1h}^X$  transition at various pressures are also plotted in Fig. 3. A linear least-squares fitting yields a pressure coefficient of  $-2.6$  meV/kbar, which is the same pressure coefficient found for the X valley in the GaAs barrier layer.<sup>24</sup>

It is well known that the  $\Gamma$  direct CB of GaAs has a positive pressure coefficient, whereas the X CB has a smaller negative one.<sup>12,13</sup> With increasing pressure, the  $\Gamma$  band edge increases and the X band edge decreases, so it is expected that the X CB crosses with the  $\Gamma$  band at high pressures. When the pressure approaches a certain critical value,  $P_c$ , where the crossover of the X CB with the first electron level confined in well layer occurs, electrons will localize in the X CB of the barrier layer, and the QW becomes a type-II heterostructure, as is schematically shown in Fig. 5. This critical pressure,  $P_c$ , can be expressed as follows:

$$P_c = \frac{E_{1h}^X(P=0) - E_{1h}^{\Gamma}(P=0, L_z)}{\alpha_W^{\Gamma} - \alpha_B^X}, \quad (2)$$

where  $\alpha_W^\Gamma$  and  $\alpha_B^X$  are the pressure coefficients of the  $\Gamma$  band of the well layer and the  $X$  band of the barrier layer, respectively, and  $E_{1h}^X$  is the photon energy of the transition from the  $X$  CB edge to the HH level at normal pressure.

When the CB crossover occurs at the pressure  $P = P_c$ , the electron wave function of the  $n = 1$  subband in a QW will have a significant overlap with that of the electron wave function in the  $X$  valley of the barrier layer, which is now located at the same energy level. As a result, an electron delocalization from the well to the barrier layer can be expected, and an additional recombination may appear, shown as  $E_{1h}^X$  in Fig. 5. Thus, the additional transition  $E_{1h}^X$  is attributed to the transition from the electron in the  $X$ -band valley of the barrier layer to the HH level in the well layer. This assertion is strongly supported by the agreement between the deduced pressure coefficient, taken from the line slope, with that of the reported value for the  $X$  CB in GaAs.<sup>24</sup> These values are substantially lower than those reported by others.<sup>12-15</sup> While it is not yet well understood, one possibility may be related to the different dependences of the confined HH level on the pressure since our pressure coefficient was determined from the  $E_{1h}^X$  transition. A spectrum taken from the ruby at high pressure ensures that the additional peaks originate only from the QW's. Since the electron and the HH are located in separate real and reciprocal spaces, the emission intensity is very weak and difficult to observe. The transfer of electrons causes the intensity of the  $E_{1h}^\Gamma$  emission to decrease drastically when the pressure exceeds  $P_c$ .

By extrapolating the  $E_{1h}^X$  line back to normal pressure, as indicated by the dashed line in Fig. 3, the transition energy from the  $X$  CB to the  $n = 1$  HH at normal pressure is deduced to be  $E_{1h}^X(P=0) = 1.920$  eV. Therefore, the VB discontinuity for the  $\text{In}_x\text{Ga}_{1-x}\text{As}/\text{GaAs}$  heterojunction is

$$\Delta E_v = E_g^X(\text{GaAs}) - [E_{1h}^X(P=0) + E_b] + E_h, \quad (3)$$

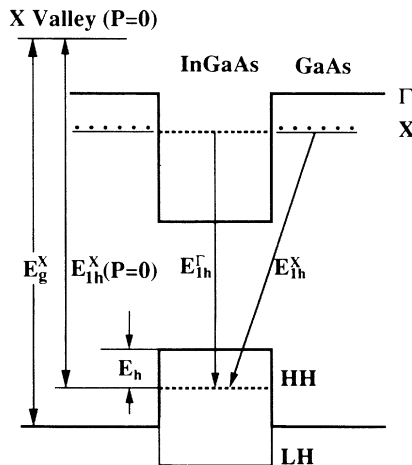


FIG. 5. Schematic diagram of the band structure at pressures  $P \geq P_c$ .

where the  $X$  CB band gap is  $E_g^X(\text{GaAs}) = 1.971$  eV,<sup>13</sup> and  $E_b$  is the binding energy of the exciton formed between the electron in the  $X$  band of the barrier and the HH level in the well layer. This exciton is labeled  $X_{1e,1h}$ . Since electrons and holes are separate in both real and reciprocal spaces, the exciton  $X_{1e,1h}$  is estimated to have  $E_b = 5$  meV.<sup>9</sup>  $E_h$  is the confinement energy of the  $n = 1$  HH in the VB quantum well. An energy-level calculation based on the envelope-function model<sup>4</sup> starting from Eq. (3) is performed. The self-consistent calculation results in a VB discontinuity,  $\Delta E_v$ , of 77 meV.

The band gap of strain-free  $\text{In}_x\text{Ga}_{1-x}\text{As}$  was calculated using the following relation:<sup>3,5</sup>

$$E_g^\Gamma(\text{In}_x\text{Ga}_{1-x}\text{As}) = E_g^\Gamma(\text{GaAs}) - 1.47x + 0.375x^2. \quad (4)$$

Furthermore, the effect of the strain on the band gap of the  $\text{In}_x\text{Ga}_{1-x}\text{As}$  layer is considered using standard elastic theory:<sup>3-6</sup>

$$\Delta E_{hh} = [-2a(C_{11} - C_{12})/C_{11} + b(C_{11} + 2C_{12})/C_{11}]\epsilon, \quad (5)$$

$$\Delta E_{lh} = [-2a(C_{11} - C_{12})/C_{11} - b(C_{11} + 2C_{12})/C_{11}]\epsilon,$$

where  $a$  and  $b$  are the deformation potentials,  $C_{11}$  and  $C_{12}$  are the elastic stiffness constants, and  $\epsilon$  is the built-in strain.

The VB offset fraction,  $Q_v = \Delta E_v / (\Delta E_v + \Delta E_c)$  is 0.32, as determined from  $\Delta E_v$  and the strained band gap of  $\text{In}_x\text{Ga}_{1-x}\text{As}$  as deduced above.  $Q_v$  has been extensively studied<sup>3-8</sup> since it is an essential parameter in the characterization of the electronic structure of semiconductor heterojunctions.  $Q_v$  has been found to be dependent of the  $\text{In}_x\text{Ga}_{1-x}\text{As}$  composition (or strain) for SQW's,<sup>7,8</sup> and our results are in reasonable agreement with reported values. The discrepancy is thought to originate from the different lineup of the band structure at the  $\text{In}_x\text{Ga}_{1-x}\text{As}/\text{GaAs}$  interfaces for samples prepared under different conditions due to indium segregation.

From Eq. (5) the splitting of HH and light-hole (LH) bands is calculated to be 120 meV for this  $x = 0.25$  sample. This value is smaller than the HH-band discontinuity, and thus the light hole is localized in the GaAs barrier layer and the heterostructure is inferred to be of type II for the LH band at this indium fraction.

### C. Dependence of the pressure coefficient on the well width

Table I shows a weak but distinguishable decrease in the pressure coefficient of the transition energy as the well widths are decreased. In order to eliminate the statistical error due to any uncertainty in deducing pressure from the ruby line, an analysis similar to Ref. 13 was applied: the energy difference between different wells at the same pressure is taken and plotted in Fig. 6 for sample 2 as a function of pressure. Least-squares fits are made using the differences in transition energies to determine the difference in the pressure coefficient instead of subtracting the individually determined pressure coefficients. Such analysis yields a slope which gives the difference in  $\alpha$  directly. As shown in Fig. 6, the slopes of the fitting lines are smaller in magnitude for pairs of quantum wells having well widths close in dimension, since their transi-

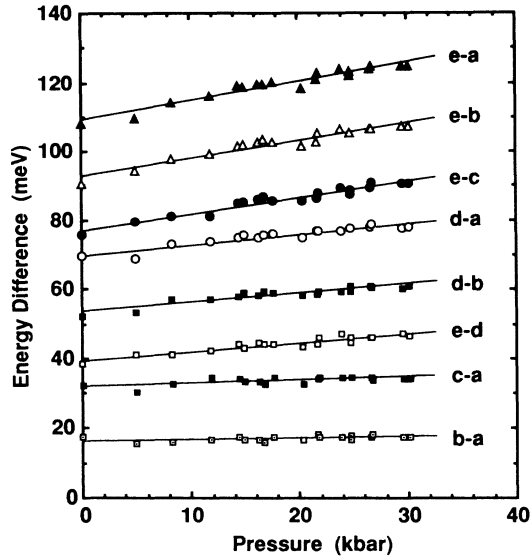


FIG. 6. Energy differences of the  $E_{1h}^{\Gamma}$  transitions for each pair of quantum wells as a function of pressure for sample 2. The lines are linear least-squares fits. Note that the magnitudes of the slopes are smaller for pairs of wells with smaller differences in transition energies.

tion energies are close in value. This kind of difference fit is made for all pairs of quantum wells in sample 2. It is clear that narrower wells have larger pressure coefficients.

Wolfold *et al.*<sup>12</sup> and Venkateswaran *et al.*<sup>13</sup> have observed that the pressure coefficient from a narrow GaAs/ $\text{Al}_x\text{Ga}_{1-x}\text{As}$  quantum well has a smaller value than that of a wide well, which is the opposite of the results presented here. There are many effects that may account for the well-width dependence of  $\alpha$ . Pressure decreases the lattice constant and therefore narrows the well width in a heterostructure. In addition, the effect of different pressure coefficients in the well and barrier layer may counter the change of the barrier height with pressure. Furthermore, the CB effective mass is increased by the application of pressure due to the nonparabolicity effect,<sup>19</sup> which affects both the subband energies and exciton binding energies in the quantum wells. Lefebvre *et al.*<sup>19</sup> have performed a calculation for GaAs/ $\text{Al}_x\text{Ga}_{1-x}\text{As}$  quantum wells based on the envelope-function model, in which the nonparabolicity of the CB was included with Kane's three-band model.<sup>19</sup> The calculation matched the experimental results<sup>13</sup> very well. Leburton *et al.* also presented similar results using different theoretical considerations.<sup>20</sup>

The same calculation made by Lefebvre and co-workers was made for the  $\text{In}_x\text{Ga}_{1-x}\text{As}/\text{GaAs}$  SQW's, and includes the consideration of the band-gap enlargement and the splitting of heavy- and light-hole bands generated by the built-in biaxial strain derived from Eq. (5). (The GaAs layer is thought to be strain free since the total thickness is much larger than that of the  $\text{In}_x\text{Ga}_{1-x}\text{As}$  layer.) The details of the calculation are not repeated here. Parameters used in this calculation are listed in

TABLE II. Physical constants of GaAs and InAs.

	GaAs	InAs
Lattice constant ( $\text{\AA}$ )	5.6533	6.0583
$C_{11}$ ( $10^{-2}$ kbar)	11.88	8.329
$C_{12}$ ( $10^{-2}$ kbar)	5.38	4.526
$a$ (eV)	-9.8	-5.9
$b$ (eV)	-1.8	-1.7
$m_c^*/m_0$	0.0665	0.023
$m_{hh}^*/m_0$	0.34	0.32
$\partial E_g/\partial P$ (meV/kbar)	10.7	9.5

Table II. Values used for the  $\text{In}_x\text{Ga}_{1-x}\text{As}$  alloy are interpolated from values for InAs and GaAs.

In Fig. 7 the theoretical result is plotted together with the experimentally determined result. The upper curve is from the calculation excluding the nonparabolicity effect of the CB, while the lower curve includes this effect using the three-band model.<sup>19</sup> In order to compare this with the experimental results, calculations are made for the different pressures at which the experiments were performed, and the final theoretical result is obtained using least-squares fitting. As shown in Fig. 7, the theoretical results are in qualitatively good agreement with the experimental results. It is found that the change in barrier height induced by the change in the pressure and the nonparabolicity of the CB are the most significant effects responsible for the  $\alpha$  dependence on the well width. The pressure coefficient of the exciton emission from the quantum well approaches that of the bulk value as the well layer approaches the wide width limit, because quantum-size effects disappear as the well width exceeds the deBroglie wavelength of the carrier. Similarly,  $\alpha$  also approaches that of the bulk value in the barrier layer as

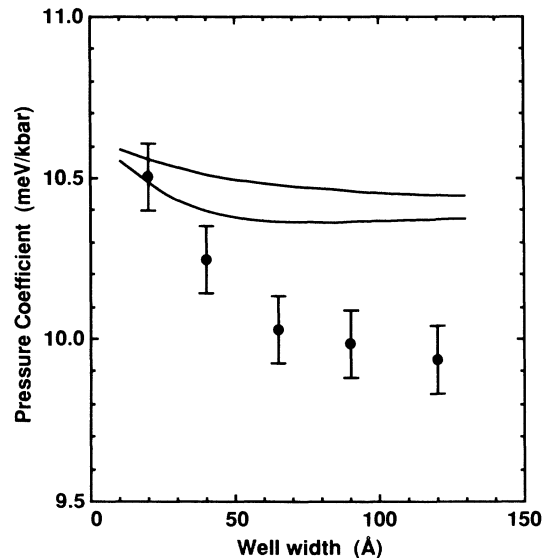


FIG. 7. Pressure coefficient as a function of the well width measured from sample 2. The curves are from the theoretical calculation using the envelope-function model: the upper curve excludes the nonparabolicity effect; the lower curve includes the nonparabolicity effect.

the well width is decreased to the *narrow* width limit, due to the extension of the exciton wave function into the barrier. Thus the wider well has a smaller  $\alpha$  since the pressure coefficient of the  $\text{In}_x\text{Ga}_{1-x}\text{As}$  well layer has a smaller value than that of the GaAs barrier layer. In GaAs/ $\text{Al}_x\text{Ga}_{1-x}\text{As}$  heterostructures,  $\alpha$  in the well layer (GaAs) is larger than that in the barrier layer ( $\text{Al}_x\text{Ga}_{1-x}\text{As}$ ),<sup>23</sup> and the tendency is, therefore, the opposite of our result.

The deviation between the experimental and theoretical results shown in Fig. 7 is not yet well understood. As can be seen in Fig. 6, the difference in transition energy subtracted from the different pairs of quantum wells is nonlinear, although there is some sublinear dependence on the pressure, which is attributed to the nonparabolicity effect of the CB. Our calculation, in which the nonparabolicity of the CB is accounted for with the three-band model,<sup>19</sup> has not yielded a significant improvement. Therefore, it seems that the three-band model does not describe the nonparabolicity of the CB well, and a more careful consideration of the strain effect may be necessary. Moreover, interactions from the *L* and *X* extrema should be considered because of pressure-induced changes to the CB configuration.<sup>15</sup>

#### IV. CONCLUSIONS

The pressure dependence of optical properties are studied for single  $\text{In}_x\text{Ga}_{1-x}\text{As}/\text{GaAs}$  strained quantum wells grown with several well widths on the same substrate, which allows for direct measurements of the pressure coefficient as a function of the well width. Pressure-dependent PL measurements, made at 77 K and up to 45 kbar, show that the transition energy is strongly dependent on the pressure. The pressure coefficient is observed to be larger for narrower wells, and this tendency is in good qualitative agreement with the envelope-function calculation. An energy crossover is observed in this material for the first time. The appearance of weak recombinations from the *X* valley in the conduction band allows for the determination of the valence-band offset rather directly.

#### ACKNOWLEDGMENTS

The authors acknowledge Y. Y. Wang, D. W. Chang, and Dr. J. Q. Liu for help in measurements, and are indebted to P. Chu for preparation of the manuscript.

\*Present address: Department of Electrical and Computer Engineering (R-007), University of California at San Diego, La Jolla, CA 92093.

<sup>1</sup>For a review, see G. C. Osbourn, P. L. Gourley, I. J. Fritz, R. M. Biefeld, L. R. Dawson, and T. E. Zipperian, *Semicond. Semimet.* **24**, 459 (1987); J. Y. Marzin *et al.*, *Superlatt. Microstruct.* **5**, 51 (1989).

<sup>2</sup>I. J. Fritz, P. L. Gourley, and L. R. Dawson, *Appl. Phys. Lett.* **51**, 1004 (1987).

<sup>3</sup>J. Y. Marzin, M. H. Charasse, and B. Sermage, *Phys. Rev. B* **31**, 8298 (1985).

<sup>4</sup>G. Ji, D. Huang, U. K. Reddy, T. S. Henderson, R. Hondre, and H. Morkoç, *J. Appl. Phys.* **62**, 3366 (1987).

<sup>5</sup>T. G. Andersson, Z. G. Chen, V. D. Kulakovskii, A. Uddin, and J. T. Vallin, *Phys. Rev. B* **37**, 4032 (1988).

<sup>6</sup>J. Menendez, A. Pinczuk, D. J. Werder, S. K. Sputz, R. C. Miller, D. L. Sivco, and A. Y. Cho, *Phys. Rev. B* **36**, 8165 (1987).

<sup>7</sup>M. J. Joyce, M. J. Johnson, M. Gal, and B. F. Usher, *Phys. Rev. B* **38**, 10978 (1988).

<sup>8</sup>H. Q. Hou, Y. Segawa, Y. Aoyagi, S. Namba, and J. M. Zhou, *Solid State Commun.* **74**, 159 (1990).

<sup>9</sup>H. Q. Hou, Y. Segawa, Y. Aoyagi, S. Namba, and J. M. Zhou, *Solid State Commun.* **70**, 997 (1989).

<sup>10</sup>E. D. Jones, H. Ackermann, J. E. Schirber, J. J. Drummond, L. R. Dawson, and I. J. Fritz, *Appl. Phys. Lett.* **47**, 492 (1985).

<sup>11</sup>L. J. Wang, H. Q. Hou, J. M. Zhou, R. M. Tang, Z. D. Lu, Y. Y. Wang, and Y. Huang, *Chin. Phys. Lett.* **6**, 67 (1989).

<sup>12</sup>D. J. Wolfold, T. F. Kuech, J. A. Bradley, M. A. Gell, D. Ninno, and M. Jaros, *J. Vac. Sci. Technol. B* **4**, 1043 (1986).

<sup>13</sup>U. Venkateswaran, M. Chandrasekhar, H. R. Chandrasekhar, B. A. Vojak, F. A. Chambers, and J. M. Meese, *Phys. Rev. B* **33**, 8416 (1986).

<sup>14</sup>D. J. Wolfold, T. F. Kuech, T. W. Steiner, J. A. Bradley, M. A. Gell, D. Ninno, and M. Jaros, *Superlatt. Microstruct.* **4**, 525 (1988).

<sup>15</sup>A. Kangarlu, H. R. Chandrasekhar, M. Chandrasekhar, Y. M. Kapoor, F. A. Chambers, B. A. Vojak, and J. M. Meese, *Phys. Rev. B* **38**, 9790 (1988).

<sup>16</sup>P. Lefebvre, B. Gil, J. Allegre, H. Mathieu, Y. Chen, and Raisin, *Phys. Rev. B* **35**, 1230 (1987).

<sup>17</sup>B. Gil, P. Lefebvre, H. Mathieu, G. Platero, M. Altarelli, T. Fukunaga, and H. Nakashima, *Phys. Rev. B* **38**, 1215 (1988).

<sup>18</sup>M. Schlierkamp, R. Wille, K. Greipel, U. Rössler, W. Schlapp, and G. Weimann, *Phys. Rev. B* **40**, 3077 (1989).

<sup>19</sup>P. Lefebvre, B. Gil, and H. Mathieu, *Phys. Rev. B* **35**, 5630 (1987).

<sup>20</sup>J. P. Leburton and K. Kahen, *Superlatt. Microstruct.* **1**, 49 (1985).

<sup>21</sup>D. Z. -Y. Ting and Yia-Chung Chang, *Phys. Rev. B* **36**, 4359 (1987).

<sup>22</sup>H. Q. Hou, Y. Huang, and J. M. Zhou, *J. Cryst. Growth* **99**, 306 (1990).

<sup>23</sup>S. Adachi, *J. Appl. Phys.* **53**, 8775 (1982); **58**, R1 (1985).

<sup>24</sup>S. Lee, J. Sanchez-Dehesa, and J. D. Dow, *Phys. Rev. B* **32**, 1152 (1985).